Chapter 1
Stress and Strain

1.1 Introduction

The opto-structural analyst is concerned with stress and deflection from externally applied loads, such as those occurring during mounting of optics, and internal loads, such as those initiated by gravity or acceleration. Additionally, the analyst is concerned with temperature change, which causes deflection and often causes stress. For cryogenic and high-temperature extremes, such values are obviously crucial; for more benign environments, temperature, loads, and self-weight deflection are still an issue, since we are concerned with fractional-wavelength-of-light changes. Accordingly, this initial chapter provides the basics of structural analysis, which lay the foundation for the chapters to follow.

1.2 Hooke's Law

Before diving into the structural analysis methods required for high-acuity optical systems, it is useful to review the origins of this analysis. While basic and advanced theories and principles of strength of materials and structural analysis have filled volumes, we review here the basis on which everything else follows. We review, therefore, the simple relation developed by Robert Hooke[1] in 1660, when he wrote *ut tensio sic vis*,[2] which literally means, "as the extension, so the force." This expression simply states that force, or load, is directly proportional to deflection for any system that can be treated as a mechanical spring, including elastic bodies, as long as such deflection is small. Simply stated,

$$F = kx, \qquad (1.1)$$

where F is the applied force, x is the resulting deflection, and k is a spring, or stiffness, constant. In this theory, the spring is fully restored to its original length upon removal of the load.

A logical extension to Hooke's law relates stress to strain in a similar fashion. Consider a bar of length L and a cross-sectional area A under an axial load P, as shown in Fig. 1.1. Here, we define stress σ as
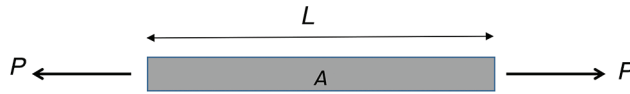
Figure 1.1   Direct tension force application to a one-dimensional (1D) element. Stress is defined as force divided by area and acts normal to the surface of the cross-section.

$$\sigma = \frac{P}{A}.$$ (1.2)

Note that this is simply a definition; stress has the units of force divided by area [MN/m^2 (MPa)], or pounds per square inch (psi).

The load in Fig. 1.1 and the resulting stress are considered to be tensile when the object is stretched and are compressive when it is shortened. Tensile and compressive stresses are called direct stresses and act normal to the cross-sectional surface.

Since stress is directly proportional to force divided by area, and strain ε (a dimensionless quantity) is related to deflection as

$$\varepsilon = \frac{x}{L},$$ (1.3)

we can now rewrite Hooke's law as

$$\sigma = E\varepsilon,$$ (1.4)

where E is a material stiffness constant; for a solid isotropic material under a unidirectional axial load, E is an inherent property of the material, called its modulus of elasticity, and often referred to as elastic modulus, tensile modulus, or Young's modulus. The modulus of elasticity has the same units as stress (psi) since strain is dimensionless.

Substituting Eq. (1.4) into Eq. (1.2), we now readily compute the axial deflection of the bar of Fig. 1.1 as

$$x = \frac{PL}{AE}.$$ (1.5)

While this formulation is quite simplified, computation of stress for 3D solids with loads in multiple directions will be more complex. To illustrate this, and for the sake of completeness, while force is a vector (it has magnitude and direction), i.e., a first-order tensor, stress is a second-order tensor, which is a multidirectional quantity, and follows a different set of rules than the simple laws of vector addition. Further, for anisotropic materials, the stiffness matrix relating stress to strain will, in general, consist of a fourth-order tensor and 21 independent terms, with Hooke's law taking the form of

$$\sigma_{ij} = \sum_{k=1}^{3} \sum_{i=1}^{3} E_{ijkl} \varepsilon_{kl}, \tag{1.6}$$

where subscripts *i*, *j* take on values of 1, 2, or 3. Fortunately, in this text, we will not make use of such advanced analyses and will need only to discuss stress and strain in two dimensions, enabling more simplified, yet accurate, analyses. In the case of isotropic loading of 3D solids, the stiffness matrix is reduced to only two quantities, *E* and *G*, the latter of which is defined as the shear modulus, or modulus of rigidity. The shear modulus *G* is related to the elastic modulus *E* as

$$G = \frac{E}{2(1 + v)}, \tag{1.7}$$

where *v* is the ratio of lateral contraction to axial elongation under axial load and varies between 0 and 0.5 for most common materials. Values of zero are common for cork, for example, and values near 0.5 are common for rubbers, which are essentially incompressible. Another way of saying this is that for a material such as rubber, its volume will be constant under load, while its volume is ever increasing as Poisson's ratio is lowered toward zero. (Theoretical values of Poisson's ratio can be as low as −1, as achieved in certain materials, and are well beyond the scope of this text).

In two dimensions,

$$E_x = \frac{(\sigma_x - v\sigma_y)}{E}, \tag{1.7a}$$

$$E_y = \frac{(\sigma_y - v\sigma_x)}{E}. \tag{1.7b}$$

Thus, for the purposes of this text, these equations are most useful and preclude the need for unwieldy, 3D constituency matrices. The introduction of the 2D effect gives rise to the additional form of Hooke's law relating to shear stress τ, given as

$$\tau = G\lambda, \tag{1.8}$$

where λ is the (dimensionless) shear strain angle.

Shear stresses act in the plane of the cross-sectional surface. For shear load force *V*, as depicted in Fig. 1.2, we find the average shear stress as

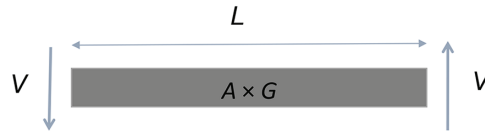$$\tau = \frac{V}{A}. \tag{1.9}$$

Figure 1.2 Direct shear force application without bending to a 1D element. Stress is defined as force divided by area and acts in the plane of the surface cross-section.

Substituting Eq. (1.8) into Eq. (1.9), we now readily compute the shear deflection (ignoring beam bending for the moment) of the bar of Fig. 1.2 as

$$y = \frac{VL}{AG}. \tag{1.10}$$

1.3 Beyond Tension, Compression, and Shear

Thus far, we have applied Hooke's law in the three translational directions: axial (x, tension/compression) and lateral (y, z, shear). There are also three rotational directions upon which bending and twist moments may act, completing the six possible degrees of freedom. Bending occurs when a moment is applied about either of the orthogonal lateral (y, z) axes, while twisting occurs when a moment [in units of inch-pounds (in.-lb)] is applied about the axial (x) axis. Figure 1.3 depicts these additional degrees of freedom. Again, in these cases, we can use Hooke's law to determine stresses and strains, and, therefore, deformation.

1.3.1 Bending stress

It is worthwhile to illustrate Hooke's law for the case of bending. Consider a beam under pure bending (constant, uniform moment), as shown in Fig. 1.4.
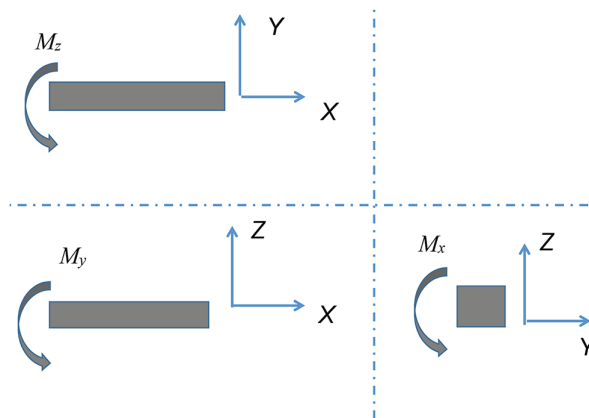

Figure 1.3 1D beam element under bending (about the z and y axes) and twist moments (about the x axis) in rotational degrees of freedom. Bending produces normal stress, while twist produces shear stress.
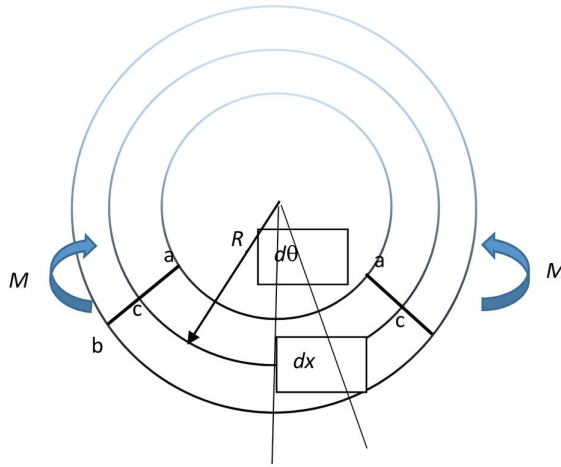
Figure 1.4 Diagram of bending stress showing section curves with radius R under moment loading. Surface a–a shortens, while surface b–b lengthens relative to neutral surface c–c.

The top (concave) surface is shortened, and the bottom (convex) surface is elongated. Somewhere in the middle there is no length change; this is the neutral axis of the beam. Since adjacent planes rotate by an amount $d\theta$, the arc length s at the neutral surface is given as

$$s = dx = Rd\theta, \tag{1.11}$$

where R is the radius of curvature of the beam.

Away from the neutral surface, the beam fibers elongate or shorten by an amount $yd\theta$, and since the original fiber length was dx, the strain is given simply as

$$\varepsilon = \pm\frac{yd\theta}{dx} = \pm\frac{y}{R}, \tag{1.12}$$

where a positive sign indicates tension, and a negative sign indicates compression. We can now apply Hooke's law (Eq. 1.4) and readily compute

$$\sigma = \frac{Ey}{R}. \tag{1.13}$$

These stresses acting over the elemental area give rise to forces that produce the resultant moment. Since there is no net force, from equilibrium it is realized that

$$\frac{E}{R}\int ydA = 0, \tag{1.14}$$

which implies that the neutral axis is at the centroid of the cross-section. The net moment M is the sum of the force distance products, or

$$M = \int y\sigma dA = \frac{E}{R} \int y^2 dA, \tag{1.15}$$

where the integral is called the area moment of inertia I of the cross-section, with dimensions of length to the fourth power. Thus, we have

$$\frac{1}{R} = \frac{M}{EI}, \tag{1.16}$$

and substitution of Eq. (1.16) into Hooke's law [Eq. (1.13)] yields

$$\sigma = \frac{My}{I}. \tag{1.17}$$

The largest value occurs as either tension or compression at the extreme fibers. Denoting the extreme fiber position as $y = c$, the maximum stress is

$$\sigma = \frac{Mc}{I}. \tag{1.18}$$

1.3.1.1 Combined normal stress

If a tensile or compressive axial load exists with a moment load, Eq. (1.18) is added to Eq. (1.2) (normal stresses acting in the same direction can be added):

$$\sigma = \frac{P}{A} + \frac{Mc}{I}. \tag{1.19}$$

It has been said that this equation is 90% of structural engineering; this is an obvious exaggeration, but the equation is, arguably, one of the most commonly used equations in structural analysis.

1.3.2 Bending deflection

For a beam of length L, it is a simple matter to compute the bending deformation y using the approximate parabolic relation

$$y = \frac{L^2}{8R}. \tag{1.20}$$

From Eq. (1.16), for a beam in pure bending,

$$y = \frac{ML^2}{8EI}. \tag{1.21}$$

Most commonly, the moment is not uniform, as is the case when transverse shear loads are introduced. Here, the curvature will vary along the beam, and differential equations—well documented in basic strength of materials literature[3] but not detailed here—give rise to deformations dependent on load and boundary conditions. For the simple case of the cantilever beam shown in Fig. 1.5, the deformation under end load *P* is

$$y = \frac{PL^3}{3EI},$$
(1.22)

and for the simply supported beam of Fig. 1.6,

$$y = \frac{PL^3}{48EI}.$$
(1.23)

Of course, deflection can be accompanied by rotation, which is the slope of the deflection curve. Table 1.1 shows the typical cases of beam deflection and rotation for various loading and support boundary conditions. Support boundary conditions can be *free*, meaning no restraint, and free to translate and rotate; *roller*, meaning free to translate in one direction but restrained in the other, and free to rotate; *pinned*, meaning restrained in translation in both directions but free to rotate; *fixed*, meaning restrained in both translation and rotation; and *guided*, meaning not free to rotate but providing for freedom to translate in one direction.

1.3.3 Shear stress due to bending

Section 1.1 presents the shear stress due to direct shear. When shear is accompanied by bending, the maximum shear stress occurs at the neutral axis and varies to zero at the free boundaries. In this case, the "average" shear
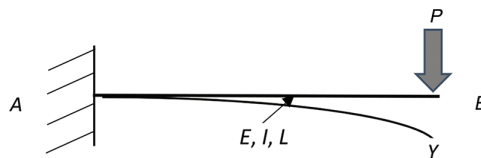

Figure 1.5   Cantilever beam bending under the end load will deflect at end B according to Eq. (1.22). There is no rotation or translation at fixed end A.
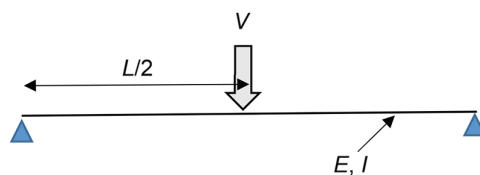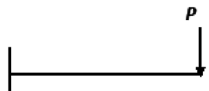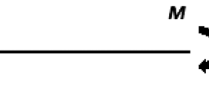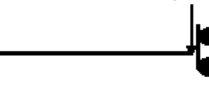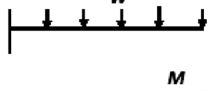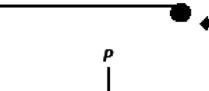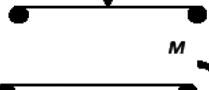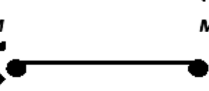

Figure 1.6   Simply supported beam bending under the central load will deflect at the center according to Eq. (1.23). There is no translation at the end points, which are allowed to rotate.

Table 1.1 Moment, deflection, and rotation for various loading and boundary conditions.

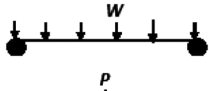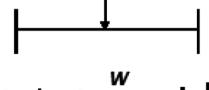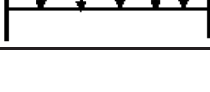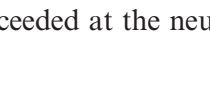|		Max. Moment	Max. Deflection	End Rotation A	End Rotation B
Cantilever end load	P	PL	$PL^3/3EI$	0	$PL^2/2EI$
Cantilever end moment	M	M	$ML^2/2EI$	0	ML/EI
Guided cantilever end load	P	$PL/2$	$PL^3/12EI$	0	0
Cantilever uniform load	W	$WL/2$	$WL^3/8EI$	0	$WL^2/6EI$
Propped cantilever end moment load	M	M	$ML^2/27EI$	0	$ML/4EI$
Simple support central load	P	$PL/4$	$PL^3/48EI$	$PL^2/16EI$	$PL^2/16EI$
Simple support end moment	M	M	$0.0612ML^2/EI$	$ML/6EI$	$ML/3EI$
Simple support end moment	M M	M	$ML^2/8EI$	$ML/2EI$	$ML/2EI$
Simple support uniform load	W	$WL/8$	$5WL^3/38EI$	$WL^2/24EI$	$WL^2/24EI$
Fixed support central load	P	$WL/8$	$WL^3/192EI$	0	0
Fixed supports uniform load	W	$WL/12$	$WL^3/384EI$	0	0

stress of Eq. (1.9) is exceeded at the neutral zone. The maximum shear stress can be computed as

$$\tau = \frac{VQ}{It},\qquad(1.24)$$

where Q is the area moment about the neutral zone and is given as

$$Q = \int y\,dA,\qquad(1.24a)$$

and t is the thickness of the cross-section at the neutral zone. Equation (1.24) can therefore be rewritten as

$$\tau = \frac{kV}{A},\tag{1.25}$$

where

$$k = \frac{AQ}{It}.\tag{1.26}$$

For the case of a rectangle,

$$\tau = \frac{3V}{2A},\tag{1.26a}$$

and for a circular cross-section,

$$\tau = \frac{4V}{3A}.\tag{1.26b}$$

1.3.4 Shear deflection due to bending (detrusion)

Similarly, Section 1.1 presents shear deflection of a beam due to direct shear. When shear is accompanied by bending, shear deflection (sometimes referred to as shear detrusion) depends on both the variation in shear across the beam and the value of Q. In the case of a pure cantilever, we modify Eq. (1.10) and find that

$$y = \frac{kVL}{AG}.\tag{1.27}$$

For other loading and boundaries where the shear varies with beam length, we can use energy methods to compute deflection. For example, for a simply supported beam under a concentrated central load (first row of Table 1.1),

$$y = \frac{kVL}{4AG}.\tag{1.28}$$

The value of k [computed in Eq. (1.26)] assumes that, in computation of shear deflection, the cross-section is free to warp. This is not the case for many conditions of loading where shear changes abruptly, as in the case of the simply supported beam with a concentrated central load. More-complex strain energy formulation shows that, in this case for a rectangular

cross-section, we find a modified coefficient as approximately $k = 6/5$, and for a circular cross-section, $k = 7/6$.

Deflection due to shear is generally small compared to deflection due to bending unless the span is short and/or the cross-section is deep. However, for lightweight optics (Chapter 6), shear deflection does have added importance.

1.3.5 Torsion

The final degree of freedom is twist about the axial axis, or torsion. Torque T (in units of pounds) is the torsional moment producing the twist. Again, Hooke's law applies, in this case, for shear [Eq. (1.8)]. Similar to what is done in bending (but not shown here), it is derived that torsional stress τ equals

$$\tau = \frac{\alpha T t}{K},\tag{1.29}$$

where α is cross-section correction constant; t is the minimum thickness dimension of the cross-section; and K, with units of length to the fourth power, is called the torsional constant. The torsional constant equals the polar moment of inertia J for a circular (solid or hollow) cross-section, where

$$J = 2I.\tag{1.30}$$

In this case, $\alpha = 0.5$ (note that t = diameter), and

$$\tau = \frac{T R}{J},\tag{1.31}$$

where R is the cross-sectional radius.

For a noncircular cross-section, the torsional constant is not the polar moment of inertia and needs a separate calculation. For a rectangular solid cross-section,

$$K = Bbt^3,\tag{1.32}$$

where b is the long-side width, and t is the short-side thickness of the section. The value of the torsional stiffness constant B is given in the plot of Fig. 1.7 as a function of the width-to-thickness ratio. Note that for thin sections, the value of B approaches 1/3.

The value for the torsional stress constant α is given in the plot of Fig. 1.8. Note that α approaches unity for a thin cross-section.

For hollow, thin-walled (t), closed, rectangular cross-sections,

$$K = \frac{4tA_0^2}{U},\tag{1.33}$$
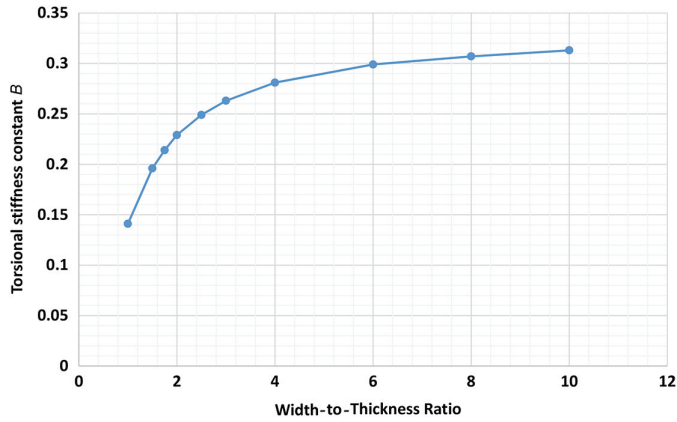
Figure 1.7   Torsional stiffness constant *B* versus width-to-thickness ratio for a rectangular cross-section. Values approach one-third for a thin cross-section.

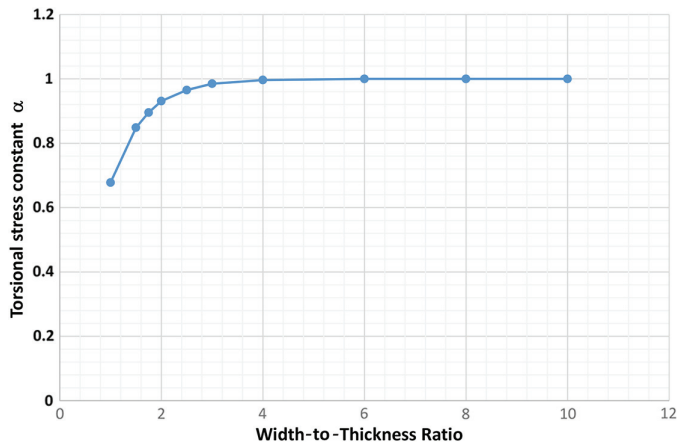**Figure 1.8**   Torsional stress constant α versus width-to-thickness ratio for a rectangular cross-section. Values approach unity for a thin cross-section.

where A_0 is the area enclosed by the mean center line of the wall, and U is the perimeter of the mean centerline of the wall.

The value of α for use in Eq. (1.29) is

$$\alpha = \frac{2A_0}{Ut},\tag{1.34}$$

from which we find that

$$\tau = \frac{T}{2A_0t}.\tag{1.35}$$

Note that for a hollow, circular cross-section, Eq. (1.35) reduces to

$$\tau = \frac{TR}{J},$$

as it must.

1.3.5.1 Twist rotation

The angle of twist is similarly derived and is given as

$$\theta = \frac{TL}{KG}, \tag{1.36}$$

where, again, K is the torsional constant depending on the cross-section as discussed above. For thin-walled sections such as channel or U shapes, the value of b can be assumed to be the total developed width of the section, to the first order. Table 1.2 summarizes the value of K for typical cross-sections.

1.3.6 Hooke's law summary

Some basic derivations using Hooke's law have been presented. While the stress and displacement calculations for more-complex situations are exhaustive if not nearly infinite (and, again, well documented in standard engineering texts and handbooks), the intent here is to set the foundation for the material that follows only as applied to opto-structural analysis. With an understanding of the basics of Hooke's law, we can better understand its more-detailed formulations.
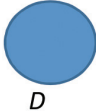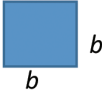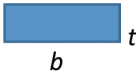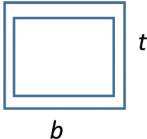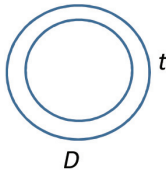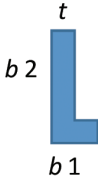
1.4 Combining Stresses

When normal (perpendicular to the area cross-section) stresses from tension, compression, or bending exist at a point, they can be combined directly. When in-plane shear stresses from torsion or direct shear exist at a point, they can be combined directly. However, as indicated in Section 1.2, stress, unlike force, is not a vector and exists in multiple orientations. Thus, when shear stresses are combined with normal stresses at a given point, they can neither be added algebraically nor vector summed, as the rules of tensor addition will apply. The addition can also be formulated by considerations of equilibrium. At any angle in a plane, the normal and shear stresses are given, respectively, as

$$\sigma = \frac{(\sigma_x + \sigma_y)}{2} + \frac{(\sigma_x - \sigma_y)}{2}\cos 2\theta - \tau_{xy}\sin 2\theta, \tag{1.37}$$

$$\tau = \frac{(\sigma_x - \sigma_y)}{2}\sin 2\theta + \tau_{xy}\cos 2\theta. \tag{1.38}$$

Table 1.2 Torsional constant *K* for various cross-sections. Dimensions of the constant are in length to the fourth power.

Section		Torsional Constant *K*
Solid circle		$\pi D^4/32$
Solid square		$0.141b^4$
Solid rectangle		(see Fig. 1.7)
Hollow square tube		b^3/t
Round tube		$\pi D^3 t/4$
Open section (thin wall)		$0.333\,(b1+b2)t^3$

Because these equations define the normal and shear stresses of a circle, a technique that uses what's called Mohr's circle is very useful in visualizing these stresses through their relationship to each other: At some angle, normal stress will be maximum and will occur where the shear stress is zero.

Differentiating Eq. (1.37) with respect to angle θ, and setting the resulting expression equal to zero (max-minima problem), we can find the angle of the maximum normal stress as

$$\tan 2\theta = \frac{2\tau}{(\sigma_x - \sigma_y)}. \tag{1.39}$$

By substitution, the maximum normal stress is calculated as

$$\sigma_1 = \frac{(\sigma_x + \sigma_y)}{2} + \sqrt{\frac{(\sigma_x - \sigma_y)^2}{4} + \tau^2} \qquad (1.40)$$

and is called the major principal stress.

The minimum stress is similarly found as

$$\sigma_2 = \frac{(\sigma_x + \sigma_y)}{2} - \sqrt{\frac{(\sigma_x - \sigma_y)^2}{4} + \tau^2} \qquad (1.41)$$

and is called the minor principal stress.

The maximum shear stress will always occur 45 deg from the principal stress angle and is calculated as

$$\tau_{\max} = \frac{(\sigma_1 - \sigma_2)}{2}. \qquad (1.42)$$

Note that the principal stress always equals or is greater than the applied normal stress and is used for determining strength.

1.4.1 Brittle and ductile materials

Principal stresses are well correlated to test strength data obtained for materials as long as they are brittle, since they generally have higher compressive strength than tensile strength. Brittle materials exhibit a low strain elongation to failure after the yield point is reached. With reference to Fig. 1.4, note that all of what has been presented applies in the linear region of a stress strain diagram, for which Hooke's law applies, i.e., below the material yield point at which it becomes nonlinear.

For ductile materials, the stresses are not conservative, and premature yielding may result. In this case, distortion energy methods are used, resulting in a maximum-stress prediction called von Mises stress. For two dimensions, von Mises stress is given as

$$\sigma_{\max} = \sqrt{\sigma_1^2 - \sigma_1\sigma_2 + \sigma_2^2} \qquad (1.43)$$

and should be used for materials that have high strain elongation before failure in yield. Note that the von Mises stress is an "equivalent" stress to be compared to the material yield strength and is not a true stress. Based on distortion theory, the premise is that the material fails by distortion, or in shear, as will be shown in the following example.

Using the von Mises criteria for the case of an object in tension (x axis only) and shear, we find from Eqs. (1.40), (1.41), and (1.43) that

$$\sigma_{\max} = \sqrt{\sigma_x^2 + 3\tau^2}. \tag{1.44}$$

Under pure shear alone,

$$\sigma_{\max} = \sqrt{3}\tau, \tag{1.45}$$

or

$$\tau = \frac{\sigma_{\max}}{\sqrt{3}} = 0.577\sigma_{\max}. \tag{1.46}$$

Thus, the distortion energy theory predicts that the shear strength is 0.577 times the tensile strength. This relation is common for most metals and other ductile isotropic materials.

A comparison of von Mises and principal stresses for typical, common 2D states of stress is given in Table 1.3.

1.5 Examples for Consideration
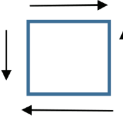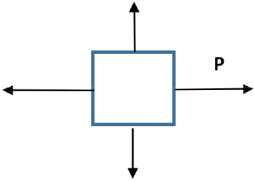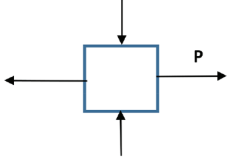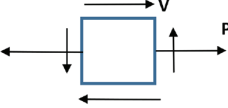
It is useful to illustrate the principles we have just discussed with some simple examples. We stress the word simple because the intent of this section is to define the basics and the basis for the material to follow. More-complex calculations will be introduced later as needed.

Example 1. Consider a beam fixed at one end (cantilevered) and loaded at its free end with an axial tensile load (x axis) of $P = 1000$ lbs and a shear Y load of $V = 2000$ lbs. The beam is 5 in. long with a rectangular cross-section of dimensions ½ in. wide by 2 in. deep. It is made of aluminum with an elastic modulus of 1.0×10^7 psi, a Poisson ratio of 0.33, and a yield strength of 35,000 psi.

Compute the following:

    a) the normal stress σ_x
    b) the shear stress τ
    c) the principal stresses σ_1, σ_2
    d) the von Mises stress $\sigma_{\max}$
    e) the maximum shear stress $\tau_{\max}$
    f) the axial displacement x
    g) the bending deflection y_b
    h) the shear deflection y_s

Table 1.3 Principal and von Mises stresses for various elemental loading types. In general, von Mises stress equals or exceeds principal stress in 2D analysis.

		Principal Stress		Von Mises Stress
		Major	**Minor**	
Uniaxial tension		1	0	1
Pure shear		1	−1	1.732
Biaxial tension		1	1	1
Tension and compression		1	−1	1.732
Uniaxial tension and shear		1.618	−0.618	2

Solutions:

a) The normal stress due to the axial load [from Eq. (1.2)] is

$$\sigma = \frac{P}{A} = \frac{1000}{1} = 1000 \, \text{psi}.$$

The normal stress due to the shear load results from the maximum bending moment, which is $M = VL$.
   The normal bending stress [from Eq. (1.18)] is

$$\sigma = \frac{VLc}{I} = \frac{6VL}{bh^2} = 7500 \, \text{psi}.$$

At a particular point at the extreme fiber, we add the normal stresses. The combined normal stress is $\sigma = 1000 + 7500 = 8500 \, \text{psi}.$

b) The shear stress [from Eq. (1.26a)] is

$$\tau = \frac{3V}{2A} = 3000 \, \text{psi.}$$

c) The major principal stress [from Eq. (1.40)] is

$$\sigma_1 = \frac{\sigma_x}{2} + \sqrt{\left(\frac{\sigma_x}{2}\right)^2 + \tau^2} = 9450 \, \text{psi,}$$

and the minor principal stress [from Eq. (1.41)] is

$$\sigma_2 = \frac{\sigma_x}{2} - \sqrt{\left(\frac{\sigma_x}{2}\right)^2 + \tau^2} = -950 \, \text{psi.}$$

d) The von Mises stress is calculated from Eq. (1.43) as

$$\sigma = \sigma_{\text{max}} = \sqrt{\sigma_1^2 - \sigma_1\sigma_2 + \sigma_2^2} = 9960 \, \text{psi.}$$

The von Mises stress is only slightly higher than the principal stress but should be used because the material is ductile.

e) The maximum shear stress is calculated from Eq. (1.42) as

$$\tau_{\text{max}} = \frac{(\sigma_1 - \sigma_2)}{2} = 5200 \, \text{psi.}$$

f) The axial displacement [from Eq. (1.5)] is

$$x = \frac{PL}{AE} = 0.0005 \, \text{in.}$$

g) The bending deflection is found from Eq. (1.22) or Table 1.1 and is

$$y_b = \frac{VL^3}{3EI} = 0.025 \, \text{in.}$$

h) The shear deflection [from Eq. (1.27)] is

$$y_s = \frac{kVL}{AG}, \quad \text{where } k = \frac{6}{5}$$
$$y_s = 0.0032 \, \text{in.}$$

The shear deflection can be added directly to the bending deflection. Note that shear deflection is typically small compared to bending deflection unless the beam length is extremely small or the cross-section is very deep.

Example 2. A cantilever beam having properties and dimensions identical to those in Example 1 above is subjected to an end torsional twist of 4000 in-lb.

Compute the following:

a) the shear stress
b) the major principal stress
c) the von Mises stress
d) the angle of twist

Solution:

a) The shear stress [from Eq. (1.29)] is given as

$$\tau = \frac{T}{\alpha b t^2} = 24800 \, \text{psi}.$$

b) The major principal stress [from Eq. (1.40)] equals the shear stress:

$$\sigma_1 = 24800 \, \text{psi}.$$

c) The von Mises stress [from Eq. (1.45)] is

$$\sigma_{\text{max}} = \sqrt{3} t = 43000 \, \text{psi}.$$

Note that the von Mises stress is significantly higher than the principal stress, and, in fact, exceeds the yield strength of the material. Since the material is ductile, the von Mises stress should be used; if the principal stress were used, a false sense of security might result, unless the user is aware that shear strength drives the design. In the latter case, if the principal stress were used, the astute analyst would check both the principal and maximum shear stresses, and would see that shear strength drives the design.

d) The angle of twist is computed from Eq. (1.36) as

$$\theta = \frac{TL}{KG} = \frac{TL}{Bbt^3} = 0.066 \, \text{rad} = 3.8 \, \text{deg}.$$

1.6 Thermal Strain and Stress

As we have seen from Hooke's law [Eqs. (1.1) and (1.4)], when an external force is applied to a member, stress is produced, and that stress is always accompanied by strain. There are cases, however, where strain is applied without producing stress, as occurs under temperature loading. Consider, for example, a beam of length L that is free to expand under a temperature excursion ΔT.

With no restraint, the beam grows an amount

$$y = \alpha L \Delta T, \tag{1.47}$$

where α is the effective thermal expansion coefficient of the material over the temperature range of interest. The beam grows according to the diagram in Fig. 1.9(a). The strain is

$$\varepsilon = \frac{y}{L} = \alpha \Delta T. \tag{1.48}$$

Because this is the natural state in which the beam occurs, there is no stress. Strain without stress is called eigenstrain.

If such a beam were completely restrained from growing [as in Fig. 1.9(b)], the amount it would naturally grow is resisted by a force, which produces stress. Thus, from Eqs. (1.5) and (1.48), we have

$$\frac{PL}{AE} = \alpha L \Delta T; \text{ therefore,}$$
$$P = AE\alpha\Delta T, \tag{1.49}$$
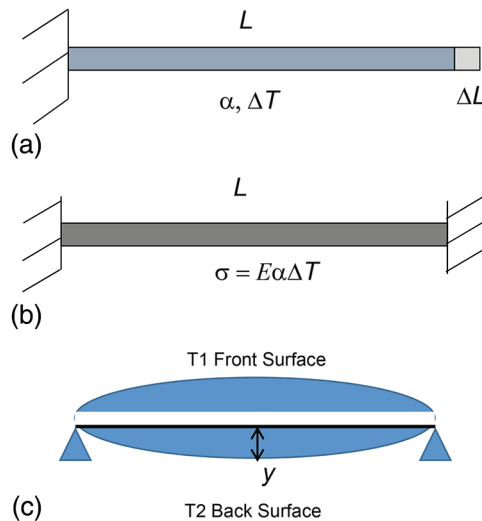
and, therefore,

(a)

(b)

(c)

Figure 1.9 Thermal expansion under uniform temperature soak of (a) a stress-free unconstrained beam and (b) a fully constrained beam inducing normal stress σ. (c) Thermal expansion of a stress-free beam simply supported at both ends with a uniform, linear, front-to-back thermal gradient.

$$\sigma = \frac{P}{A} = E\alpha\Delta T. \tag{1.50}$$

This simple equation is very important (because stress developed under thermal strain when constrained will rarely exceed this amount) and serves as an upper bound for first-order calculations. Along with Eq. (1.18), Eq. (1.50) is one of the simplest and most important relationships in opto-structural analysis. (Chapter 4 will expand on this in two dimensions).

Note that the resisting force is independent of length, and the developed stress is independent of both length and cross-sectional area, which is nice. Note further that if a member wants to expand and is not free to do so, the force and stress are in compression; if it wants to shrink and is not free to do so, it is in tension.

Similarly, consider a case in which a thermal gradient is applied through the depth of the cross-section. For a linear gradient, we have again a case of eigenstrain if the beam is unrestrained, and it will bend without stress to the shape shown in Fig. 1.9(c). Here, the radius (of the neutral axis) is

$$R = \frac{t}{\alpha\Delta T}. \tag{1.51}$$

For a positive expansion coefficient and a positive temperature change on the top surface, the top tends to expand and bend the beam in a convex direction. Again, if the beam is fully constrained, stress will develop with the top surface in compression. (In thermal cases, you sometimes have to think backward.) The developed stress for the fully constrained case is

$$\sigma = \frac{E\alpha\Delta T}{2}. \tag{1.52}$$

Note again, in this case, that the stress is independent of length and cross-sectional area or bending (area moment of) inertia. This is nice. We will expand on this in Chapter 4, where we will also discuss nonlinear gradients, which do require cross-sectional knowledge. At this point, we have simply set the stage for the more-detailed analyses that follow.

1.6.1 Thermal hoop stress

A common example of thermal stress occurs when two rings of differing coefficients of thermal expansion (CTEs) are in contact in a thermal environment, resulting in an interference that produces hoop stress in both components, as shown in Fig. 1.10. Hoop stress σ is given as

$$\sigma = \frac{qR}{A}, \tag{1.53}$$
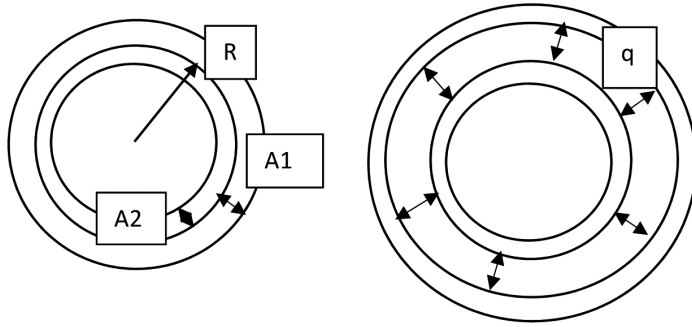
Figure 1.10 Diagram illustrating hoop stress. Two rings of unit width and constant thickness (A1 and A2) produce self-equilibrating pressure *q* when subjected to a temperature change for given properties of modulus *E* and differing thermal expansion coefficients α.

where R is the mean ring radius at contact, q is the induced interference pressure in pounds per inch, and A is the cross-sectional area of the individual rings. What remains is to solve for q under a thermal soak condition. From Hooke's law, the induced circumferential strain is

$$\varepsilon = \frac{\sigma}{E} = \frac{qR}{AE}. \tag{1.54}$$

The thermal strain is simply $\Delta\alpha\Delta T$, in which

$$\Delta\alpha = \alpha_1 - \alpha_2,$$

where the subscript numbers denote the outer and inner rings, respectively. From compatibility, we have

$$\alpha_1\Delta t - \frac{qR}{(AE)_1} = \alpha_2\Delta t + \frac{qR}{(AE)_2}. \tag{1.55}$$

Solving for q, we obtain

$$q = \frac{\Delta\alpha\Delta T(AE)_2}{\left[1 + \frac{(AE)_2}{(AE)_1}\right]R}. \tag{1.56}$$

The stress is recovered from Eq. (1.53).

Note that if the inner ring is very stiff relative to the outer ring, $(AE)_2$ is set to infinity in Eq. (1.55), and

$$q = \frac{(AE)_1\Delta\alpha\Delta T}{R}. \tag{1.57}$$

The outer ring stress [from Eq. (1.53)] is

$$\sigma = \frac{qR}{A} = E_1 \Delta\alpha\Delta T \qquad (1.58)$$

independent of both A and R.

1.6.1.1 Solid disk in ring

In the case of a circular, solid disk—as in an optical lens radially restrained in a cell—the induced stress is uniform throughout; i.e., its principal stress is identical at any point. Here, the lens strain is

$$\varepsilon = \frac{\sigma}{E} = \frac{q}{Eb}, \qquad (1.59)$$

and the induced stress is thus

$$\sigma = E\varepsilon = \frac{q}{b}. \qquad (1.60)$$

Therefore, under thermal soak, we can modify Eq. (1.55) to yield

$$\Delta\alpha\Delta T = \frac{qR}{tbE_1} + \frac{q}{E_2 b}, \qquad (1.55a)$$

where the subscripts 1 and 2 denote the ring and disk, respectively. Hence, Eq. (1.56) can be written as

$$q = \frac{\Delta\alpha\Delta T}{\left(\frac{R}{tbE_1} + \frac{1}{E_2 b}\right)}. \qquad (1.56a)$$

Note from Eq. (1.56a) that if the disk is very rigid relative to the ring, then the ring stress is

$$\sigma = E_1 \Delta\alpha\Delta T \qquad (1.58a)$$

independent of the radius, and the disk stress is

$$\sigma = \frac{E_1 t \Delta\alpha\Delta T}{R}, \qquad (1.60a)$$

which is *inversely proportional* to the radius.

Note from Eq. (1.56a) that if the ring is very rigid relative to the disk, then the ring stress is

$$\sigma = \frac{E_2 \Delta \alpha \Delta T R}{t} \qquad (1.58b)$$

directly proportional to the radius, and the disk stress is

$$\sigma = E_2 \Delta \alpha \Delta T \qquad (1.60b)$$

independent of the radius.

Example. We can apply these relationships to the case of a lens cell housing an optical lens. Consider a zinc sulfide lens 1 in. deep b and 4 in. in diameter encased in a 1-in.-deep by 0.10-in.-thick t aluminum lens housing. Over a soak from room temperature to 150 K, compute the stress in the lens and housing. The following effective properties over the range of soak are given:

$$E_1 = 9.9 \times 10^6 \text{psi}$$
$$E_2 = 1.08 \times 10^7 \text{psi}$$
$$\alpha_1 = 2.10 \times 10^{-5}/\text{K}$$
$$\alpha_2 = 5.6 \times 10^{-6}/\text{K}$$

Since the lens is rigid relative to the housing, we find from Eq. (1.57), where $A = bt$, that

$$q = \frac{(1)(0.1)(9.9)(15.4)(143)}{2} = 1100 \,\text{lb/in.},$$

and the housing stress from Eq. (1.58) is

$$\sigma = (9.9)(15.4)(143) = 21800 \,\text{psi}.$$

The line pressure q on the lens is the same as that on the housing, and the lens stress, under uniform principal stress everywhere throughout, is recovered from Eq. (1.60) as

$$\sigma = \frac{q}{b}; \text{ therefore,}$$

$$\sigma = \frac{1100}{1} = 1100 \,\text{psi}.$$

1.6.2 Ring in ring in ring

Similar to the thermal stress induced by the interference of two rings, it is useful to review the case of thermal interference involving three rings. This could occur, for example, when a thin isolation ring is housed between an optic with a central hole and housing, or an insert is bonded to a housing. In this case, we need to consider the strain compatibility relationships between the inner and middle rings, and between the central and outer rings. This is a
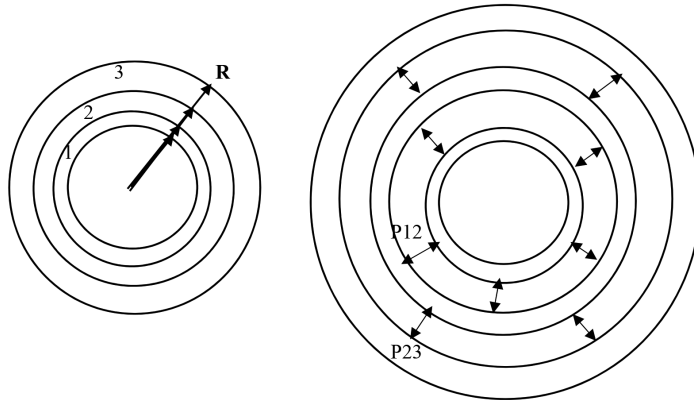
Figure 1.11   Ring-in-ring-in-ring hoop stress. Each ring has an inner and outer radius *R*, and each can have different modulus, thickness, and expansion characteristics. Expansion leads to self-equilibrating pressure on each surface.

bit more complex than the two-ring problem. Figure 1.11 is a schematic of the three-ring design, along with an equilibrium diagram. In this case, we need not limit thickness to thin rings. Using thick-ring theory,[4] and after tedious calculations, we arrive at the individual ring stresses. We compute both radial and hoop stresses for a total of 12 stresses. (Because the inner and outer radial stresses are always zero, there are ten calculable stresses.) These stresses are given in Table 1.4, and the numerous constants are defined in Table 1.5. These constants are readily programmable to the stress equations of Table 1.4 by use of a spreadsheet. Table 1.6 gives the material property constants used for computation of the hoop and radial stresses defined in Table 1.5.

When the outermost (or innermost) ring is not present and the rings are thin, the problem reduces to the simplified two-ring case of Eqs. (1.53) and (1.56) (believe it or not) with an error difference of less than 5%.

Table 1.4   Tri-ring hoop and radial stresses. Subscripts 1, 2, and 3 refer to inner, middle, and outer rings, respectively; subscripts o and i refer to outer and inner surfaces respectively; *r* is the radius at the specified interface; other constants are from Table 1.5.

σ_{r1i}	Radial stress inner surface inner ring	0
$\sigma_{\theta 1i}$	Hoop stress inner surface inner ring	$-2p_{12}r_{1o}^2/A_{1m}$
σ_{r1o}	Radial stress outer surface inner ring	$-p_{12}$
$\sigma_{\theta 1o}$	Hoop stress outer surface inner ring	$-p_{12}A_{1p}/A_{1m}$
σ_{r2i}	Radial stress inner surface middle ring	$-p_{12}$
$\sigma_{\theta 2i}$	Hoop stress inner surface middle ring	$(p_{12}A_{2p} - 2p_{23}r_{2o}^2)/A_{2m}$
σ_{r2o}	Radial stress outer surface middle ring	$-p_{23}$
$\sigma_{\theta 2o}$	Hoop stress outer surface middle ring	$(2p_{12}r_{2i}^2 - 2p_{23}A_{2p})/A_{2m}$
σ_{r3i}	Radial stress inner surface outer ring	$-p_{23}$
$\sigma_{\theta 3i}$	Hoop stress inner surface outer ring	$p_{23}A_{3p}/A_{3m}$
σ_{r3o}	Radial stress outer surface outer ring	0
$\sigma_{\theta 3o}$	Hoop stress outer surface outer ring	$2p_{23}r_{3i}^2/A_{3m}$

Table 1.5 Constants used for computation of the hoop and radial stresses defined in Table 1.4. ΔT = temperature soak.

A_{1p}	Geometry constant	$r_{1o}^2 + r_{1i}^2$
A_{1m}	Geometry constant	$r_{12o}^2 - r_{12i}^2$
A_{2p}	Geometry constant	$r_{2o}^2 + r_{2i}^2$
A_{2m}	Geometry constant	$r_{2o}^2 - r_{2i}^2$
A_{3p}	Geometry constant	$r_{3o}^2 + r_{3i}^2$
A_{3m}	Geometry constant	$r_{3o}^2 - r_{3i}^2$
c_1	Geometry/material constant	$r_{2i}(A_{2p}/A_{2m} + \upsilon_2)/E_2 + r_{1o}(A_{1p}/A_{1m} - \upsilon_1)/E_1$
c_2	Geometry/material constant	$-2r_{2i}r_{2o}^2/(E_2 A_{2m})$
c_3	Geometry/material constant	$-2r_{2i}^2 r_{2o}/(E_2 A_{2m})$
c_4	Geometry/material constant	$r_{3i}(A_{3p}/A_{3m} + \upsilon_3)/E_3 + r_{2o}(A_{2p}/A_{2m} - \upsilon_2)/E_2$
d_{12}	Interference inner to middle ring	$\Delta T(-r_{2i}\alpha_2 + r_{1o}\alpha_1)$
d_{23}	Interference middle to outer ring	$\Delta T(-r_{3i}\alpha_3 + r_{2o}\alpha_2)$
p_{12}	Pressure inner to middle ring	$(c_4 d_{12} - c_2 d_{23})/(c_1 c_4 - c_2 c_3)$
p_{23}	Pressure middle to outer ring	$d_{12}/c_2 - c_1 p_{12}/c_2$

Table 1.6 Material property constants used for computation of the hoop and radial stresses defined in Table 1.5.

E_1	Young's modulus inner ring	Input
υ_1	Poisson's ratio inner ring	Input
α_1	CTE inner ring	Input
E_2	Young's modulus middle ring	Input
υ_2	Poisson's ratio middle ring	Input
α_2	CTE middle ring	Input
E_3	Young's modulus outer ring	Input
υ_3	Poisson's ratio outer ring	Input
α_3	CTE outer ring	Input

1.6.2.1 Case study

Consider a silicon optic with a central hole. The optic is supported by an aluminum hub ring that is rigidly attached by a relatively soft isolation ring of Vespel®, as shown in Fig. 1.12. The assembly is subjected to a soak change of 100 °C. For the dimensions shown, determine the stress in the optic. The effective properties over the thermal range are given in Table 1.7. The maximum hoop stress is obtained from Tables 1.4 through 1.6 as

$$\sigma_{\theta 3i} = \frac{p_{23} A_{3p}}{A_{3m}} = 5360 \, \text{psi}.$$

Note that, while this stress level may be well below the allowable value for polished silicon, it would be problematic if excessively deep flaws were present, as discussed in Chapter 12.
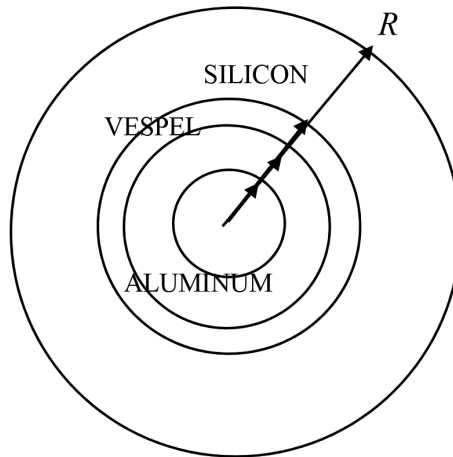
Figure 1.12   Diagram of the case study setup: an aluminum hub is placed in the central hole of a silicon optic that is isolated with Vespel and undergoes a temperature soak to 100 °C. Properties and dimensions are the same as those in the example in Section 1.6.1.1.

Table 1.7   Material and dimensional properties for the case study.

| | | | | Radius | |
| | | | | **Inner** | **Outer** |
Material	**Modulus**	**Poisson's Ratio (psi)**	**CTE (ppm/°C)**	**(inch)**	**(inch)**
Aluminum	1.00E+07	0.33	2.15E-05	5	5.50
Vespel	4.70E+05	0.35	4.00E-05	5.5	5.75
Silicon	1.90E+07	0.2	2.00E-06	5.75	8.00

1.6.3 Nonuniform cross-section

The previous discussion of a uniform cross-section shows thermal stress independent of cross-section or length, approaching the maximum of Eq. (1.50). However, for a nonuniform cross-section, this is not the case.

Consider, for example, the trapped 1D beam of Fig. 1.13 in which the cross-section varies and undergoes a temperature change of ΔT. As it becomes warmer, the beam tends to expand stress free as

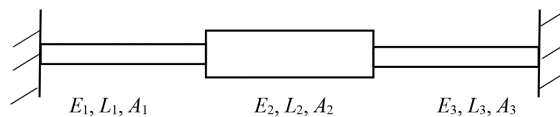$$y = \Sigma \alpha_i L_i \Delta T. \tag{1.61}$$

Figure 1.13   A fixed beam with nonunform properties subjected to temperature soak can produce extreme stress conditions.

The rigid wall will not let it expand and pushes back with compressive force P. Since the net deflection is zero, we have, from Hooke's law,

$$P\left[\Sigma\left(\frac{L_i}{A_1 E_1}\right)\right] = \Sigma \alpha_i L_i \Delta T \tag{1.62}$$

so that

$$P = \frac{\Sigma \alpha_i L_i \Delta T}{\left(\Sigma \frac{L_i}{A_1 E_1}\right)},$$

and

$$\sigma = \frac{P}{A_i}. \tag{1.63}$$

For the case shown in Fig. 1.13, we have

$$P = \frac{(2\alpha_1 L_1 + \alpha_2 L_2)\Delta T A_1 A_2 E_1 E_2}{(2L_1 A_2 E_2 + L_2 A_1 E_1)}, \tag{1.64}$$

and

$$\sigma_1 = \frac{P}{A_1} = \frac{(2\alpha_1 L_1 + \alpha_2 L_2)\Delta T A_2 E_1 E_2}{(2L_1 A_2 E_2 + L_2 A_1 E_1)}, \tag{1.65a}$$

$$\sigma_1 = \frac{P}{A_2} = \frac{(2\alpha_1 L_1 + \alpha_2 L_2)\Delta T A_1 E_1 E_2}{(2L_1 A_2 E_2 + L_2 A_1 E_1)}. \tag{1.65b}$$

Note that, unlike the uniform-cross-section case, stress is now dependent on both area and length.

For the beam of Fig. 1.13, in which the modulus and CTE are constant but the section length and the individual cross-sectional areas vary, we let $\beta = A_2/A_1$ and $\gamma = L_2/L_1$, and substituting into Eq. (1.64), find that

$$\sigma_2 = \frac{2 + \gamma}{2\beta + \gamma} E\alpha\Delta T. \tag{1.66}$$

For equal-length sections ($L_1 = L_2$), if the central cross-section is significantly smaller than the end cross-sections, its stress approaches

$$\sigma_2 = \frac{P}{A_2} = 3E\alpha\Delta T, \tag{1.67}$$

which is in considerable excess of that for the uniform case of Eq. (1.50).

   Should the thermal stress exceed the yield point of a particular ductile material, the material will not necessarily fail as long as the thermal strain lies under the material elongation capability. It will, however, be in a yielded state, which may require consideration for critical performance criteria. Also, if the load is compressive, buckling can occur, as discussed in the next section.

1.7 Buckling

This introductory chapter concludes with a note on critical buckling. Buckling occurs when a compressive axial load reaches a certain limit, causing instability. It occurs in long, slender beams. We concentrate here on 1D instability, although buckling can certainly occur in plates and shells, which are cases beyond the scope of what is presented here.

   Consider the beam of Fig. 1.14 axially loaded along the x axis in compression. If a small load or displacement is applied laterally at the location of the axial load, the beam bends slightly. If the lateral load is removed, the beam returns to its straight position. However, if the axial load is increased, now causing an increased moment due to the lateral eccentricity, the beam becomes unstable and does not return to its straight position when the lateral load is removed. If the axial load increases further, the beam displacement becomes very large, and the beam becomes unstable. This load is called the critical buckling load. Note that this phenomenon will only occur in compression, as tensile loading will serve to straighten any eccentric lateral displacement.

   We can compute the critical load by using the bending and curvature relations of Section 1.3 [Eq. (1.16)] and Fig. 1.4 to determine the point of instability. Here, we see that
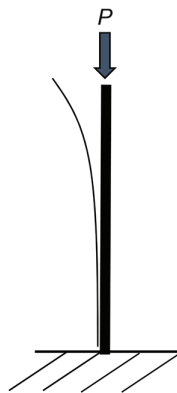

Figure 1.14   Critical buckling instability occurs at a critical load in compression due to small lateral movement. The joint at the application of the load may be free, pinned, or fixed with axial motion allowed. The base can be pinned or fixed. The critical load depends on these boundary conditions.

$$M = \frac{EI}{R} = EI\frac{d^2y}{dx^2} = P(\delta - y). \tag{1.68}$$

This differential equation is readily solved by calculus techniques[3] to produce the critical load value at instability as

$$P_{cr} = \frac{\pi^2 EI}{4L^2}. \tag{1.69}$$

The solution is independent of the material strength and is only a function of its stiffness.

While Eq. (1.69) is solved for the cantilever case, where critical value is the lowest possible, solutions are found for varying boundary conditions. If the beam is simply supported at its ends, the critical load is

$$P_{cr} = \frac{\pi^2 EI}{L^2}. \tag{1.70}$$

If it is fixed at both ends, the load is

$$P_{cr} = \frac{4\pi^2 EI}{L^2}, \tag{1.71}$$

which is the other extreme, so we have bounded the problem.

For many applications in optical structures, buckling needs to be investigated as it may drive the design, even if stress values are below those allowable. We will see an example of this in Chapter 3.

References

1. R. Hooke, *Lectures of Spring*, Martyn, London (1678).
2. R. Hooke, "A Latin (alphabetical) anagram, *ceiiinosssttuv*," originally stated in 1660 and published 18 years later.
3. S. Timoshenko and D. Young, *Strength of Materials*, Fourth Edition, D. Van Nostrand Co., New York (1962).
4. R. J. Roark and W. C. Young, *Formulas for Stress and Strain*, Fifth Edition, McGraw-Hill, New York, p. 504 (1975).